



*Research article*

# Imaging dose of cone-beam computed tomography in nanoparticle-enhanced image-guided radiotherapy: A Monte Carlo phantom study

Dewmini Mututantri-Bastiyange<sup>1</sup> and James C. L. Chow<sup>2,3,\*</sup>

<sup>1</sup> Department of Physics, Ryerson University, Toronto, ON, M5B 2K3 Canada

<sup>2</sup> Radiation Medicine Program, Princess Margaret Cancer Centre, University Health Network, Toronto, ON, M5G 1X6 Canada

<sup>3</sup> Department of Radiation Oncology, University of Toronto, Toronto, ON, M5T 1P5 Canada

\* **Correspondence:** Email: james.chow@rmp.uhn.ca; Tel: +4169464501; Fax: +4169466566.

**Abstract:** Using kilovoltage cone-beam computed tomography (kV-CBCT) and heavy-atom radiosensitizers in image-guided radiotherapy (IGRT) can provide numerous benefits, such as image contrast enhancement in radiation dose delivery. However, the increased use of kV-CBCT for daily imaging procedures may inevitably deposit certain amount of radiation dose to the patient, especially when nanoparticles used as radiosensitizers are involved. In this study, we use Monte Carlo simulation to evaluate the imaging dose escalation due to nanoparticle addition with varying nanoparticle material, nanoparticle concentration and photon beam energy. A phantom was used to determine the relationships between the imaging dose enhancement ratios (IDERs) and different concentrations (3–40 mg/ml) of gold (Au), platinum (Pt), iodine (I), silver (Ag) and iron oxide (Fe<sub>2</sub>O<sub>3</sub>) nanoparticles, under the delivery of 120–140 kVp photon beams from the CBCT. It is found that gold and platinum nanoparticles of 40 mg/ml concentration had the highest IDER (~1.6) under the 120 kVp photon beam. This nanoparticle addition resulted in a 0.63% increase of imaging dose based on a typical dose prescription of 200 cGy per fraction in radiotherapy, and is within the standard uncertainty of  $\pm 5\%$  in radiation dose delivery. This study proves that the incorporation of higher concentration nanoparticles under lower photon beam energy could increase the imaging dose. The results from this study can enable us to understand more about the incorporation of heavy-atom nanoparticles in IGRT systems.

---

**Keywords:** nanoparticles; image contrast; imaging dose; Monte Carlo simulation; cone-beam CT

---

## 1. Introduction

Radiotherapy is a method to treat both benign and malignant tumours. Currently, it accounts for about 50% of cancer treatment procedures [1]. Radiotherapy depends on the direct deposition of energy into the tumour. The reproduction of cancer cells stops due to several types of DNA damage, such as double-strand break, which is caused by the deposition of energy from radiation [2–4]. Hence therapeutic radiation has the ability to slow tumour growth and attempt to keep it stagnant. The main goal of radiotherapy is to deliver dose that is distributed over the entire tumour, while avoiding the irradiation of surrounding healthy tissues. External-beam radiotherapy delivers dose to the patient from the outside using therapeutic radiation, and the accuracy achievable is limited as a result of patient mobility and the variation in position of the targeted volumes [5]. Hence, radiation delivery methods incorporating imaging techniques that allow a deeper assessment of the target volumes and locality of tumours need to be utilized.

Over the past 20–30 years, the progress in diagnostic imaging has led to the improvement of momentary and spatial characterization of tumours at the time of radiotherapy. The state-of-the-art imaging modality such as cone-beam computed tomography (CBCT) has been incorporated into current treatment machines [6,7]. This is known as image-guided radiotherapy (IGRT) [8,9]. The guidance from the imaging enables radiotherapy to accommodate any changes in the shape, size and position of the tumour and surrounding tissues that may occur during treatment. The introduction of IGRT has allowed for greater accuracy in determining the tumour location and therefore has improved the radiation dose delivery. Despite the fact that the concept of combining imaging technologies and treatment machines being fairly new, there has been rapid growth in the enforcement and availability of IGRT systems. IGRT implements various imaging techniques by utilizing modalities ranging from ultrasonography [10] to kilovoltage CBCT (kV-CBCT) [11]. The kV-CBCT is generally installed in a medical linear accelerator. Integration of kV-CBCT into treatment machine provides tremendous benefit because it produces 3D visuals of the target and organs-at-risk prior to the initiation of radiotherapy while the patient is positioned to receive the treatment. Hence the implication of IGRT has greatly improved the accuracy of dose delivery. Moreover, implementation of IGRT can be the ideal system to maximize the impact of radiosensitizers that have been introduced into the field of radiotherapy [12,13].

In radiotherapy, the benefits of heavy-atom nanoparticles as radiosensitizers to enhance dose and image contrast are taken into great consideration, and it is an emerging field in medical imaging and biomedical engineering [14–16]. Nanoparticles have the capability of detecting cancer due to the leaky nature of tumour blood vessels, which enables nanoparticles to penetrate and accumulate in the tumour because of their small size [17–19]. Heavy-atom nanoparticles have a high mass energy absorption coefficient because they have high atomic numbers. Since the photoelectric effect contributes mainly to the photon beam attenuation at kV energy range, adding nanoparticles to the patient can enhance the image contrast in kV-CBCT and improve the accuracy in radiation dose delivery [12,20]. However, such nanoparticle addition at the same time increases the imaging dose of the patient, which should be avoided and kept to the minimum. It is because this unnecessary radiation exposure may produce adverse and side effects to the patient in radiotherapy [21,22].

In this study, we focused on the increase of imaging dose with the incorporation of heavy-atom nanoparticles in the kV-CBCT guided radiotherapy. This is particularly important because variations of higher imaging doses are anticipated due to the increase in the photoelectric effect caused by the kV photon beam, predominantly when using heavy-atom or high atomic number materials. Although there are studies on the imaging dose estimation with variations of photon beam energy from the CBCT, and patient setup uncertainty without nanoparticle addition using Monte Carlo simulation [23–25], there is no related study on the increase of imaging dose due to applying nanoparticles as contrast agent in the CBCT imaging. In this current investigation, photon beams from the CBCT with various energies of 120, 130 and 140 kVp were simulated using Monte Carlo method [14]. This was performed to make accurate calculations of imaging dose enhancement for a phantom based on patient geometry and configuration with the addition of various nanoparticle concentrations in an IGRT system. The aims of this work were to (1) provide, in detail, the relationship between the imaging dose enhancement and nanoparticle materials such as gold, platinum, iodine, silver and iron oxide incorporated into the phantom; (2) evaluate the relationship between the imaging dose enhancement and various nanoparticle concentrations; and (3) investigate the relationship between the imaging dose enhancement and various photon beam energies from the CBCT with nanoparticle addition.

## 2. Materials and method

### 2.1. Imaging dose enhancement ratio

The increase of imaging dose in nanoparticle-enhanced IGRT can be calculated by the imaging dose enhancement ratio (IDER) as follows:

$$IDER = \frac{D_{(water+nanoparticles)}}{D_{(water)}} \quad (1)$$

where  $D_{(water + nanoparticles)}$  is the imaging dose of the phantom with nanoparticles added to the tumour and normal tissue (water equivalent), and  $D_{(water)}$  is the imaging dose of the phantom without nanoparticle addition. Both phantoms with and without nanoparticle addition were irradiated by the photon beam from the CBCT using the same beam geometry, setting and beam-on time. The value of IDER informed us the increase of imaging dose due to the nanoparticle addition in IGRT. When there is no nanoparticle added to the phantom, the IDER is equal to one.

### 2.2. Monte Carlo simulation

The photon beam produced by the kV-CBCT was modeled by Monte Carlo simulation, with phase-space files containing particle information of type, orientation and energy, using the EGSnrc-based BEAMnrc code [26,27]. In this study, the conventional kV X-ray tube (Cornet DX-9, Cornet AG, Bern, Switzerland) in the X-ray volume imaging CBCT system associated with an Elekta Synergy linear accelerator was modeled. Three photon beams from the CBCT with energies of 120, 130 and 140 kVp were simulated with a projection area of  $41 \times 41 \text{ cm}^2$  at a distance of 153.6 cm from the source, based on the clinical CBCT image acquisition protocol in IGRT [23]. Each phase-space file contained 100 million particles and the photon beam model was verified by

experimental dosimetry elsewhere using the NACP parallel plate ionization chamber and MedTec water phantom [23,24].

An oval shaped phantom with a horizontal radius of 28 cm and vertical radius of 20 cm, mimicking a patient's pelvis was used in this study [23]. Monte Carlo simulations on the phantom irradiated by a 360 degree photon arc with energy equal to 120, 130 and 140 kVp were carried out using the EGSnrc-based DOSXYZnrc code [28]. The simulation setup of the phantom and CBCT X-ray source is shown in Figure 1. Characteristics and energy spectra for different photon beam energies of CBCT were studied elsewhere [29]. In the simulation using the kV photon beam, the atomic relaxation, Rayleigh scattering, electron impact ionization, bound Compton scattering and spin effect were included. The transport of Auger and Coster-Kronig electrons were also considered. Moreover, since the low-photon energies' electrons were not transported, the energy cutoff of the electron and photon transport was set to 521 keV and 1 keV in the simulation to achieve a reasonable computing time.

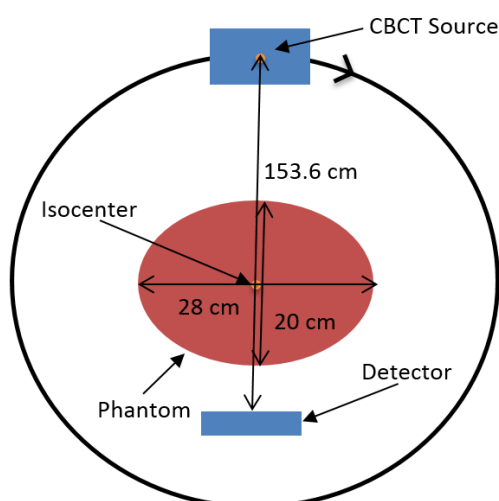


**Figure 1.** Schematic diagram showing the simulation setup of the phantom and CBCT X-ray source.

Radiation dose deposited to the phantom from the CBCT was predicted with or without the addition of the heavy-atom nanoparticles to the phantom. In the simulations, different nanoparticles of gold (Au), platinum (Pt), iodine (I), silver (Ag) and iron oxide ( $\text{Fe}_2\text{O}_3$ ) were added to the phantom with concentration varying from 3 to 40 mg/ml, and the imaging doses of the 120, 130 and 140 kVp photon beams from the CBCT were determined. By calculating the IDER as functions of nanoparticle material, nanoparticle concentration and photon beam energy, dependences of the above variables on the increase of imaging dose in nanoparticle-enhanced IGRT can be predicted.

### 3. Results and discussion

#### 3.1. Dependence of imaging dose enhancement on nanoparticle material

Figure 2 shows the dependence of IDER on nanoparticle material using nanoparticles with

increasing concentration and photon beams from the CBCT. Figure 2A–C presents the IDERs for the 120, 130, and 140 kVp photon beam, respectively, for different nanoparticle concentrations. Figure 2 shows that the IDER for all nanoparticles differ under the delivery of different photon beams. The highest IDER values resulted for gold and platinum nanoparticles. However, it is noted that platinum nanoparticles were slightly higher than gold nanoparticles. These results held true for all the kVp photon beams from the CBCT. For the rest of the nanoparticles, it is found that the IDER values for the iodine and silver nanoparticles were not as close as platinum and gold values. However the difference was not that great compared to iron oxide. In Figure 2, for all concentrations, the lowest values resulted for iron oxide.

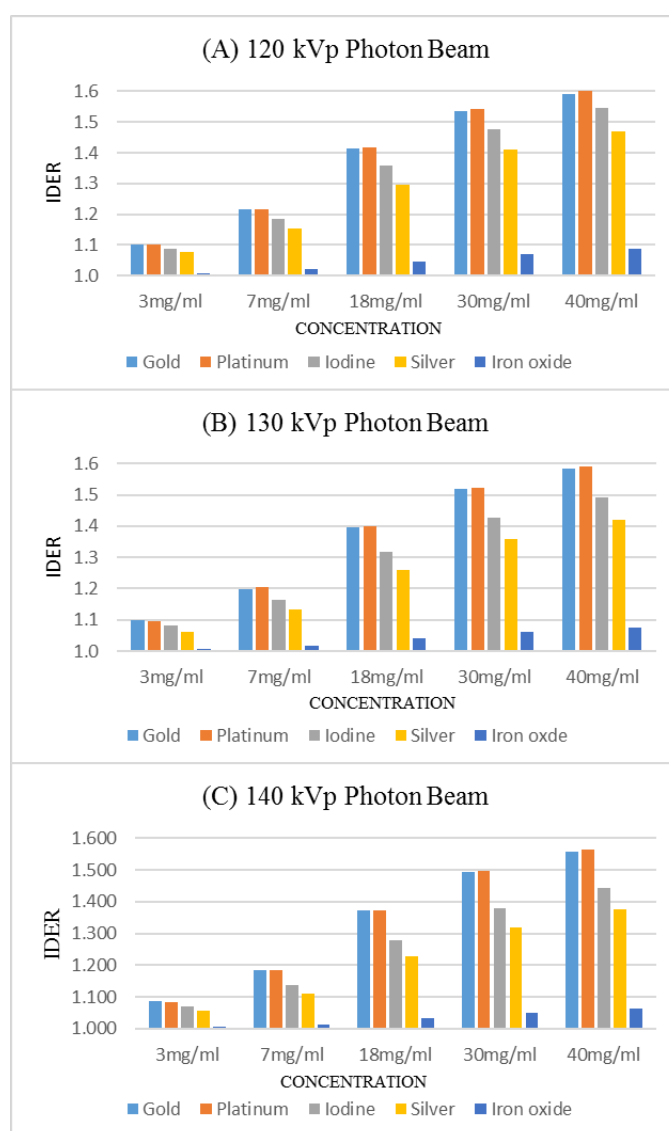


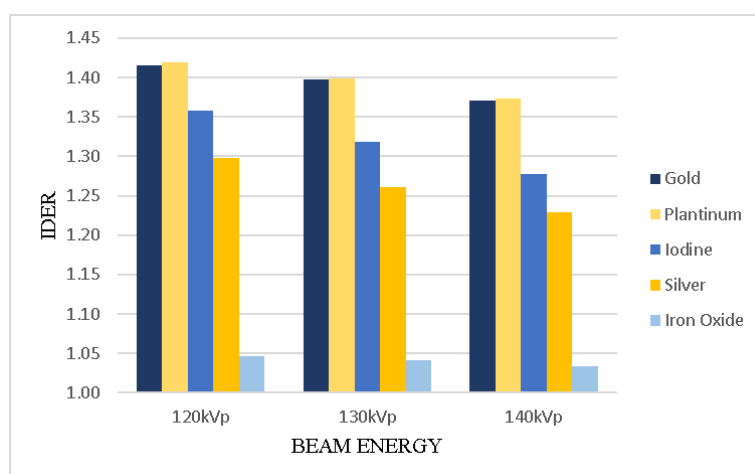
**Figure 2.** Relationship between the IDER and different nanoparticle concentrations with the delivery of (A) 120, (B) 130, and (C) 140 kVp photon beam from the CBCT.

It can be seen in Figure 2 that apart from gold and platinum (which have very close atomic numbers of 79 and 78, respectively), a clear relationship between the atomic number of a material

and IDER values was evident: as the atomic number of the material in the phantom increased the IDER values also increased. This result is reasonable because the greater the atomic number of materials in a medium is, the higher the chances of photoelectric effect taking place in the kV beam energy range, thus the higher attenuation X-rays experience when passing through the medium [30].

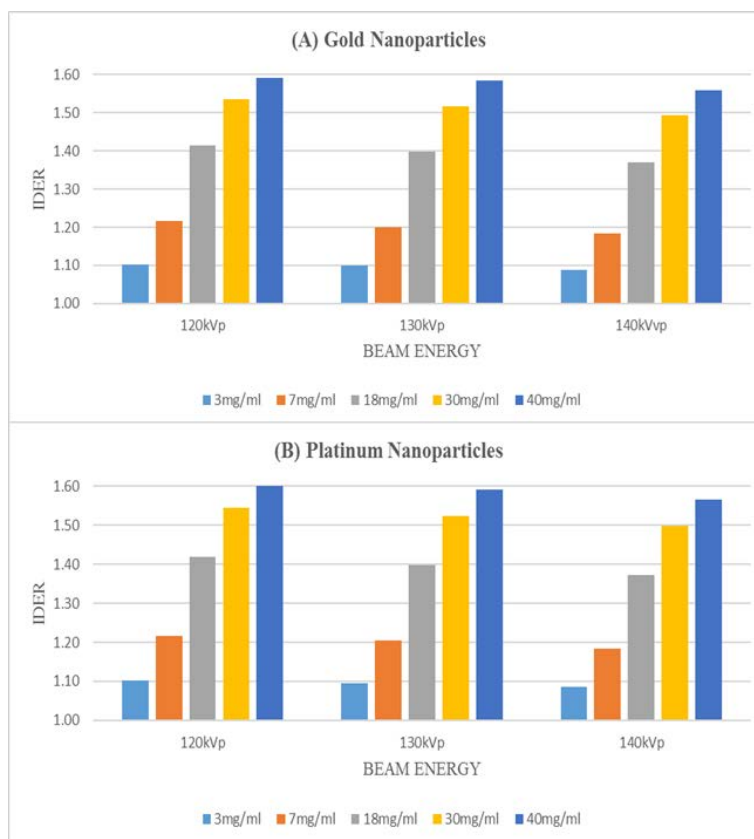
### 3.2. Dependence of imaging dose enhancement on photon beam energy

Figure 3 shows the dependence of IDER on different photon beam energy varying with nanoparticle material. In Figure 3, the nanoparticle concentration is equal to 18 mg/ml.



**Figure 3.** Relationship between the IDER and photon beam energy delivered to the phantom with 18 mg/ml concentration of different nanoparticles.

It is seen in Figure 3 that the IDER values for all nanoparticles and photon beam energies were larger than one. This means that adding nanoparticles to the phantom (i.e. water and nanoparticles) increases the imaging dose compared to the phantom alone (i.e. water). This is due to the increase of compositional atomic number of the phantom, when heavy-atom nanoparticles were added, as the cross-section of the photoelectric effect increases with the atomic number of material. In addition, for all nanoparticles, for the lower beam energy of 120 kVp, the IDER was much higher in comparison to IDER values attained for 130 and 140 kVp beam energies. In Figure 3, the IDER value using the 120 kVp photon beam for gold nanoparticles was 1.42 whereas the IDER value with the 130 kVp photon beam was just 1.39. Similarly, the two IDER values determined for platinum nanoparticles were 1.42 and 1.39 for the 120 kVp and 130 kVp photon beam, respectively. It is obvious that the lower the photon beam energy, the higher the resulting IDER value, and this relationship is seen for all concentrations of gold and platinum as shown in Figure 4, respectively. Moreover, in Figures 3 and 4, it is seen that the lower the photon beam energy is, the higher the corresponding values for IDER. This result can be explained by the photoelectric effect because higher energy photon beams (e.g. 130 and 140 kVp) are less likely to interact with matter and the heavy-atom nanoparticles, hence leading to less attenuation and less imaging dose deposited to patients [31]. Low-energy kV beams (e.g. 120 kVp), on the other hand, interact more with matter and heavy-atom nanoparticles, which result in more attenuation thus giving rise to a higher imaging dose.



**Figure 4.** Relationship between the IDER and kV photon beam energy delivered to a phantom with different concentrations of (A) gold and (B) platinum nanoparticles.

### 3.3. Dependence of imaging dose enhancement on nanoparticle concentration

Figure 5 shows the IDER values calculated for the imaging dose of phantom combined with various concentrations of (A) gold and (B) platinum nanoparticles using the 120–140 kVp photon beams. In Figure 5, it is apparent that as the nanoparticle concentration increased from 3 to 40 mg/ml, the resulting IDER values for the gold and platinum nanoparticles increased. For gold nanoparticles, in the delivery of 120 kVp photon beam, nanoparticle concentrations of 3, 7, 18, 30, and 40 mg/ml resulted in the corresponding IDER values of 1.10, 1.22, 1.41, 1.53, and 1.59, respectively. Likewise, under the same photon beam energy, the values of IDER for platinum nanoparticles with concentrations ranging from 3 to 40 mg/ml were calculated as 1.10, 1.21, 1.41, 1.54 and 1.60. These results can be explained because when there is an increase in the nanoparticle concentration, there is a greater accumulation of higher numbered atomic particles within the tumour and normal tissues, which correspondently has the ability to attenuate a greater degree of the incident photon beams. This trend was apparent for all five nanoparticle materials in this study, thus providing the evidence to support the relationship between the nanoparticle concentration present within the phantom and the resulting IDER. Moreover, there was not a single aberration that differed from the expected trend, implying that for every nanoparticle material the IDER always increased with increasing nanoparticle concentration.

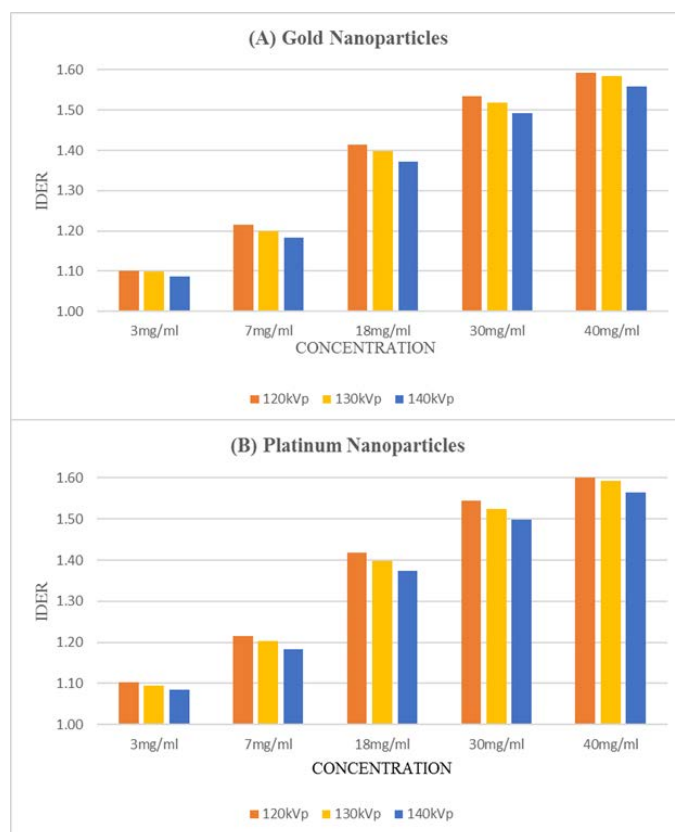


**Figure 5.** Relationship between the IDER and different concentrations of (A) gold and (B) platinum nanoparticles irradiated by different kV photon beams from the CBCT.

#### 3.4. Imaging dose escalation due to heavy-atom nanoparticle addition

From the Monte Carlo results of IDER, both gold and platinum nanoparticles performed the best in the image contrast enhancement for the kV photon beams from the CBCT. However, at the same time, they contributed the highest imaging dose escalation in the nanoparticle-enhanced IGRT. For the highest nanoparticle concentration of gold and platinum nanoparticles, the maximum IDER values are 1.59 and 1.60, respectively. That is, the imaging dose will be increased by 59% and 60% if gold and platinum nanoparticles are used as radiosensitizers in IGRT. The typical imaging dose of CBCT is about 2.1 cGy per fraction regarding our phantom type from experimental dosimetry [32]. Adding gold or platinum nanoparticles in IGRT would increase the imaging dose of about 1.26 cGy, which was about 0.63% of the prescription dose of a typical radiation dose delivery (200 cGy/fraction). This dose escalation is within the standard of uncertainty in radiation dose delivery equal to  $\pm 5\%$  [33]. On the contrary, using nanoparticles with lower atomic number will reduce the imaging dose, but it will also reduce the image contrast enhancement in IGRT.

#### 3.5. Potential clinical implementation and future study

It is seen from Section 3.1–3.4 that the performance of the nanoparticle contrast agent depends on a number of variables, namely, nanoparticle concentration, nanoparticle material, CBCT beam energy and the imaging dose [34]. Optimizing the performance of CBCT imaging with heavy-atom



nanoparticles requires intensive research efforts in the preclinical and clinical level [35]. It is expected that Monte Carlo simulation can work out the optimal balance among various radiosensitizing properties in the nanoparticle-enhanced image-guided radiotherapy with less experimental resources. To conveniently determine the imaging dose using a macroscopic approach, the popular EGSnrc code was used in the dose prediction. For future work, other Monte Carlo codes such as PENELOPE should be considered for a comparison of particle transport model and benchmarking [36].

#### 4. Conclusion

The increase of imaging dose from the CBCT in nanoparticle-enhanced IGRT was determined using Monte Carlo simulation. The IDERs were calculated as a function of photon beam energy, nanoparticle material and concentration. It was apparent that both the gold and platinum nanoparticles had similar IDER values overall. In addition, through this study it was ascertained that the higher the nanoparticle concentration, the higher the IDER there will be; and the lower the photon beam energy, the higher the imaging dose will be. Considering the maximum IDER of 1.6 for platinum nanoparticles with concentration of 40 mg/ml using the 120 kVp photon beam in this study, the increase of imaging dose was only about 0.63% to the prescription dose of 200 cGy in one fraction of radiotherapy. This is within the uncertainty of a clinical radiation dose delivery ( $\pm 5\%$ ). This study provided new information on imaging dose escalation in nanoparticle-enhanced IGRT, which showed its dependence on different nanoparticle variables such as concentration and material.

#### Acknowledgments

The authors would like to thank Xiao J. Zheng from Ryerson University to prepare the database for the heavy-atom nanoparticles used in Monte Carlo simulation.

#### Conflict of interest

The authors have no potential conflict of interest on financial or commercial matters associated with this study.

#### References

1. Zubizarreta E, Van Dyk J, Lievens Y (2017) Analysis of global radiotherapy needs and costs by geographic region and income level. *Clin Oncol* 29: 84–92.
2. He C, Chow JCL (2016) Gold nanoparticle DNA damage in radiotherapy: A Monte Carlo study. *AIMS Bioeng* 3: 352–361.
3. Berbeco RI, Korideck H, Ngwa W, et al. (2012) DNA damage enhancement from gold nanoparticles for clinical MV photon beams. *Radiat Res.* 178: 604–608.
4. Boudaïffa B, Cloutier P, Hunting D, et al. (2000) Resonant formation of DNA strand breaks by low-energy (3 to 20 eV) electrons. *Sci* 287: 1658–1660.

5. Killoran JH, Kooy HM, Gladstone DJ, et al. (1997) A numerical simulation of organ motion and daily setup uncertainties: implications for radiation therapy. *Int J Radiat Oncol Biol Phys* 37: 213–221.
6. Jaffray DA, Siewerdsen JH, Wong JW, et al. (2002) Flat-panel cone-beam computed tomography for image-guided radiation therapy. *Int J Radiat Oncol Biol Phys* 53: 1337–1349.
7. Groh BA, Siewerdsen JH, Drake DG, et al. (2002) A performance comparison of flat-panel imager-based MV and kV cone-beam CT. *Med Phys* 29: 967–975.
8. Jaffray DA (2012) Image-guided radiotherapy: from current concept to future perspectives. *Nat Rev Clin Oncol* 9: 688–699.
9. Chen GTY, Sharp GC, Mori S (2009) A review of image-guided radiotherapy. *Radiol Phys Tech* 2: 1–12.
10. van der Meer S, Bloemen-van Gorp E, Hermans J, et al. (2013) Critical assessment of intramodality 3D ultrasound imaging for prostate IGRT compared to fiducial markers. *Med Phys* 40: 071707.
11. Boda-Heggemann J, Lohr F, Wenz F, et al. (2011) kV cone-beam CT-based IGRT. *Strahlenther Onkol* 187: 284–291.
12. Abdulle A, Chow JCL (2019) Contrast enhancement for portal imaging in nanoparticle-enhanced radiotherapy: A Monte Carlo phantom evaluation using flattening-filter-free photon beams. *Nanomaterials* 9: 920.
13. Nagesha DK, Tada DB, Stambaugh CKK, et al. (2010) Radiosensitizer-eluting nanocoatings on gold fiducials for biological in-situ image-guided radio therapy (BIS-IGRT). *Phys Med Biol* 55: 6039.
14. Chow JCL (2018) Recent progress in Monte Carlo simulation on gold nanoparticle radiosensitization. *AIMS Biophys* 5: 231–244.
15. Chow JCL (2017) Application of nanoparticle materials in radiation therapy, In: Martínez LMT, Kharissova OV, Kharisov BI, *Handbook of Ecomaterials*, Switzerland: Springer, 1–21.
16. Chow JCL (2018) Monte Carlo nanodosimetry in gold nanoparticle-enhanced radiotherapy, In: Chan MF, *Recent Advancements and Applications in Dosimetry*, New York: Nova Science Publishers.
17. Reuveni T, Motiei M, Romman Z, et al. (2011) Targeted gold nanoparticles enable molecular CT imaging of cancer: an in vivo study. *Int J Nanomed* 6: 2859–2864.
18. Hepel M, Stobiecka M (2012) Detection of oxidative stress biomarkers using functional gold nanoparticles, In: Matijević E, *Fine Particles in Medicine and Pharmacy*, Boston: Springer, 241–281.
19. Stobiecka M, Ratajczak K, Jakiela S (2019) Toward early cancer detection: Focus on biosensing systems and biosensors for an anti-apoptotic protein survivin and survivin mRNA. *Biosens Bioelectron* 137: 58–71.
20. Leung MKK, Chow JCL, Chithrani BD, et al. (2011) Irradiation of gold nanoparticles by x-rays: Monte Carlo simulation of dose enhancements and the spatial properties of the secondary electrons production. *Med Phys* 38: 624–631.
21. Bertelsen A, Schytte T, Bentzen SM, et al. (2011) Radiation dose response of normal lung assessed by Cone Beam CT—a potential tool for biologically adaptive radiation therapy. *Radiother Oncol* 100: 351–355.

22. Stock M, Palm A, Altendorfer A, et al. (2012) IGRT induced dose burden for a variety of imaging protocols at two different anatomical sites. *Radiother Oncol* 102: 355–363.
23. Chow JCL, Leung MKK, Islam MK, et al. (2008) Evaluation of the effect of patient dose from cone beam computed tomography on prostate IMRT using Monte Carlo simulation. *Med Phys* 35: 52–60.
24. Chow JCL (2009) Cone-beam CT dosimetry for the positional variation in isocenter: A Monte Carlo study. *Med Phys* 36: 3512–3520.
25. Jia X, Yan H, Gu X, et al. (2012) Fast Monte Carlo simulation for patient-specific CT/CBCT imaging dose calculation. *Phys Med Biol* 57: 577.
26. Kawrakow I (2001) The EGSnrc code system, Monte Carlo simulation of electron and photon transport. NRCC Report Pirs-701.
27. Rogers DWO, Walters B, Kawrakow I (2009) BEAMnrc Users Manual. NRCC Report Pirs-509.
28. Walters B, Kawrakow I, Rogers DWO (2005) DOSXYZnrc Users Manual. NRCC Report Pirs-794.
29. Ding GX, Coffey CW (2010) Beam characteristics and radiation output of a kilovoltage cone-beam CT. *Phys Med Biol* 55: 5231–5248.
30. Albayedh F, Chow JCL (2018) Monte Carlo simulation on the imaging contrast enhancement in nanoparticle-enhanced radiotherapy. *J Med Phys* 43: 195–199.
31. Chow JCL (2016) Photon and electron interactions with gold nanoparticles: A Monte Carlo study on gold nanoparticle-enhanced radiotherapy. *Nanobiomater Med Imaging* 8: 45–70.
32. Alaei P, Spezi E (2015) Imaging dose from cone beam computed tomography in radiation therapy. *Phys Med* 31: 647–658.
33. Brahme A (1988) Accuracy requirements and quality assurance of external beam therapy with photons and electrons. *Acta Oncol* 27: 1–76.
34. Schuemann J, Berbeco R, Chithrani DB, et al. (2016) Roadmap to clinical use of gold nanoparticles for radiation sensitization. *Int J Radiation Oncol Biol Phys* 94: 189–205.
35. Hainfeld JF, Slatkin DN, Focella TM, et al. (2006) Gold nanoparticles: a new X-ray contrast agent. *Br J Radiol* 79: 248–253.
36. Casanelli B, Santibáñez M, Valente M (2020) Particle size effect on fluorescence emission for Au-infused soft tissues, *Rad Phys Chem* 167: 108302.



AIMS Press

© 2020 the Author(s), licensee AIMS Press. This is an open access article distributed under the terms of the Creative Commons Attribution License (<http://creativecommons.org/licenses/by/4.0>)